

Supporting information

Eco-friendly NaCl glycerol-based deep eutectic electrolyte for high-voltage electrochemical double layer capacitor

Daniele Motta^a, Alessandro Damin^a, Hamideh Darjazi^{b,c}, Stefano Nejrotti^a, Federica Piccirilli^{d,e}, Giovanni Birarda^d, Claudia Barolo^{a,c}, Claudio Gerbaldi^{b,c}, Giuseppe Antonio Elia^{b,c}, Matteo Bonomo^{a,c,f,}*

^a Department of Chemistry, NIS Interdepartmental Centre and INSTM Reference Centre, Università di Torino, Torino 10135, Italy

Email: daniele.motta@unito.it; alessandro.damin@unito.it; stefano.nejrotti@unito.it;
claudia.barolo@unito.it; matteo.bonomo@unito.it

^b GAME Lab, Department of Applied Science and Technology – DISAT, Politecnico di Torino, Torino 10129, Italy

Email: hamideh.darjazi@polito.it; giuseppe.elia@polito.it; claudio.gerbaldi@polito.it

^c National Reference Center for Electrochemical Energy Storage (GISEL) – INSTM, Firenze 50121, Italy

^d Elettra Synchrotron Light Laboratory, Basovizza 34149, Trieste, Italy

Email: federica.piccirilli@elettra.eu; giovanni.birarda@elettra.eu

^e Area Science Park, Padriciano 34149, Trieste, Italy

^f Department of Basic and Applied Sciences for Engineering (SBAI), Sapienza Università di Roma, Roma 00139, Italy

* Corresponding author: matteo.bonomo@unito.it

Mixture	Molar ratio	Water content	
		ppm	% w/w
NaCl-EG	1:18	655	0.07
	1:16	491	0.05
	1:14	532	0.05
	1:12	518	0.05
NaCl-Gly	1:14	1557	0.16
	1:12	1472	0.15
	1:10	1385	0.14
	1:8	1193	0.12

Table S1. Water content of formulated mixtures measured with Karl Fischer coulometric titration.

Mixture	Molar ratio	Melting temperature	
			°C
Pure Gly	/	17.8	
Pure EG	/	-12.9	
NaCl-Gly	1:14	-16.0 ± 0.6	
	1:12	-16.7 ± 0.3	
	1:10	-18.3 ± 0.3	
	1:8	-15.0 ± 0.9	
NaCl-EG	1:18	-20.0	
	1:16	-20.7	
	1:14	-21.2	
	1:12	-21.6	

Table S2. Experimental melting temperatures of NaCl-Gly mixtures (*ad hoc* method) and NaCl-EG mixtures (DSC analysis).

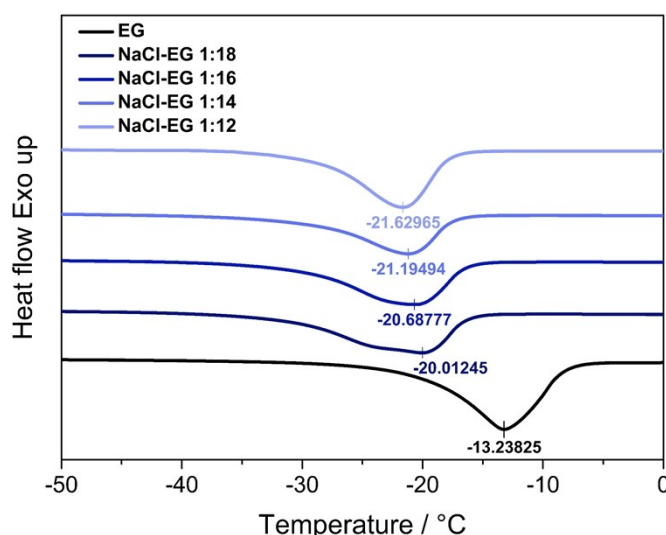


Figure S1. Melting temperatures of EG-based mixtures recorded with DSC analysis.

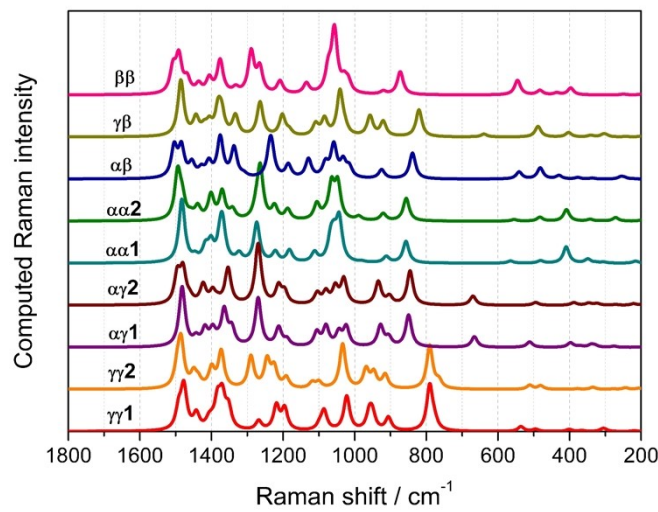


Figure S2. Raman spectra of Gly conformers from 200 to 1800 cm^{-1} simulated using EG as implicit solvent.

All the calculations (structures optimization and computation of vibrational frequencies, together with Raman spectra) were performed by means of the Gaussian 16 code¹ at the B3LYP-D3-bj^{2–6} level of theory (a fine grid has been used for the integral evaluation). Basis set for describing H, C, and O atoms was the standard Pople 6-31+G(2d,p). Finally, solvent (ethylene glycol, hereafter EG) effects were included through the SMD variation of IEFPCM 6 as developed in the Gaussian16 code and without changing the default settings.

Conformers	Raman shift / cm^{-1}
ββ	873
γβ	820
αβ	838
αα2	856
αα1	857
αγ2	845
αγ1	849
γγ2	790
γγ1	790

Table S3. Raman shifts of C-C stretching for each conformer from the simulated spectra.

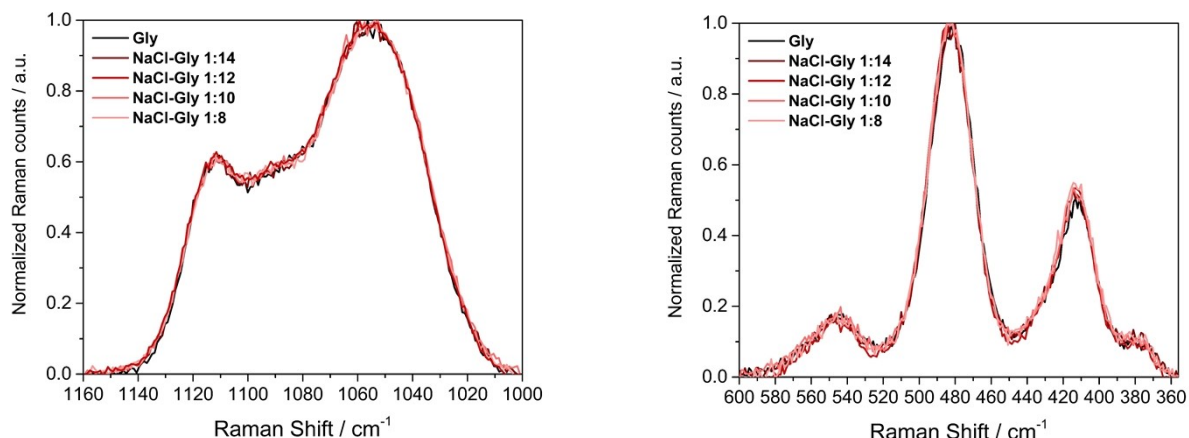


Figure S3. Raman spectra in the C-O stretching (1000-1160 cm⁻¹) and C-C-O rocking (356-600 cm⁻¹) regions of Gly-based mixtures spectra.

Raman shift / cm ⁻¹	Assignment
328	Intermolecular H-bond
415	C-C-O rocking
485	C-C-O rocking
548	C-C-C bending
673	O-H bending or C-C-O bending
819	C-C stretching
852	C-C stretching
925	CH ₂ rocking
976	CH ₂ rocking
1054	C-O stretch (terminal C)
1092	CH ₂ twisting
1115	C-O stretch (central C)
1203	CH ₂ twisting
1256	CH ₂ twisting
1314	CH ₂ twisting
1342	C-O-H bending
1466	CH ₂ scissoring

Table S4. Principal bands of glycerol in the region 100-1800 cm⁻¹ according to ⁷.

Spectroscopic characterization of NaCl-Gly mixtures

Ethylene glycol molecules exhibit conformational degrees of freedom, due to the central O-C-C-O dihedral and the two terminal dihedrals, H-O-C-C and C-C-O-H. The combination of different rotation angles in the molecule allows the EG to show up in 27 possible conformations, of which 10 are unique⁸. For simplicity authors generally divide the conformations in two groups, *gauche* and *trans*, relying on the central O-C-C-O dihedral (without accounting the terminal dihedrals H-O-C-C and C-C-O-H), allowing an easier spectroscopic rationalization. Moreover, the molecular dynamics simulations conducted by Jindal *et al.*⁹ have demonstrated that in the liquid state of EG the central O-C-C-O exists for 80% in gauche conformation and for 20 % in *trans* conformation. Principal bands in the region 100-1800 cm⁻¹ are listed in Table S5. A noteworthy aspect that is noticeable from the spectrum of the pure solvent in Figure S4, is that the intensity of the band at 482 cm⁻¹ (C-C-O bending *trans*) is greater than the intensity of the band at 523 cm⁻¹ (C-C-O bending *gauche*). Indeed, since the C-C-O bending of the *trans* conformation is more Raman active, as expected by the higher symmetry of the molecule, the *gauche* conformer presents a less intense band, even though it is four times more present in the liquid form. After the addition of NaCl into the EG some regions of the spectrum (Figure S4) undergo significant variations. The regions 450-580 cm⁻¹ and 810-920 cm⁻¹ were investigated since they are sensitive to the population of conformers and to the interaction between the metal and the glycolic hydroxy-groups, respectively. Indeed, Williams *et al.*¹⁰ reported an investigation of the interactions between salts, based on chloride and bivalent metals, and a solution of ethylene glycol in water. This study attributed changes in the region between 800 and 900 cm⁻¹ to the type of coordination between metal and glycolic hydroxy-groups. In this region, there is a strong band at 865 cm⁻¹ due to the C-C stretching, together with a C-O stretching component, and a shoulder at 884 cm⁻¹ due to CH₂ rocking vibration, coupled with the C-O stretching motion. The higher is the concentration of a metal capable of performing bidentate coordination, the more pronounced is this shoulder. On the contrary, metals which form monodentate coordination cause a minor change in the spectrum. Observing the experimental spectra of the mixtures (Figure S4), the difference in the shoulder at 884 cm⁻¹ can be immediately noticed, but this is not very pronounced and therefore the coordination is monodentate. Given the presence of two conformations (*gauche* and *trans*) in the liquid phase of EG, an analogue analysis was carried out in the region 450-580 cm⁻¹, where the bands are ascribable to C-C-O bending. As Figure S4 shows, the band at 480 cm⁻¹, relating to the C-C-O bending of the *trans* conformation, decreases as the NaCl concentration increases, while the band at 521 cm⁻¹, relating to the *gauche* conformation, increases as the NaCl concentration increases. This suggests that the addition of the salt induces structural change of the solvent, although these do not lead to the formation of a eutectic system.

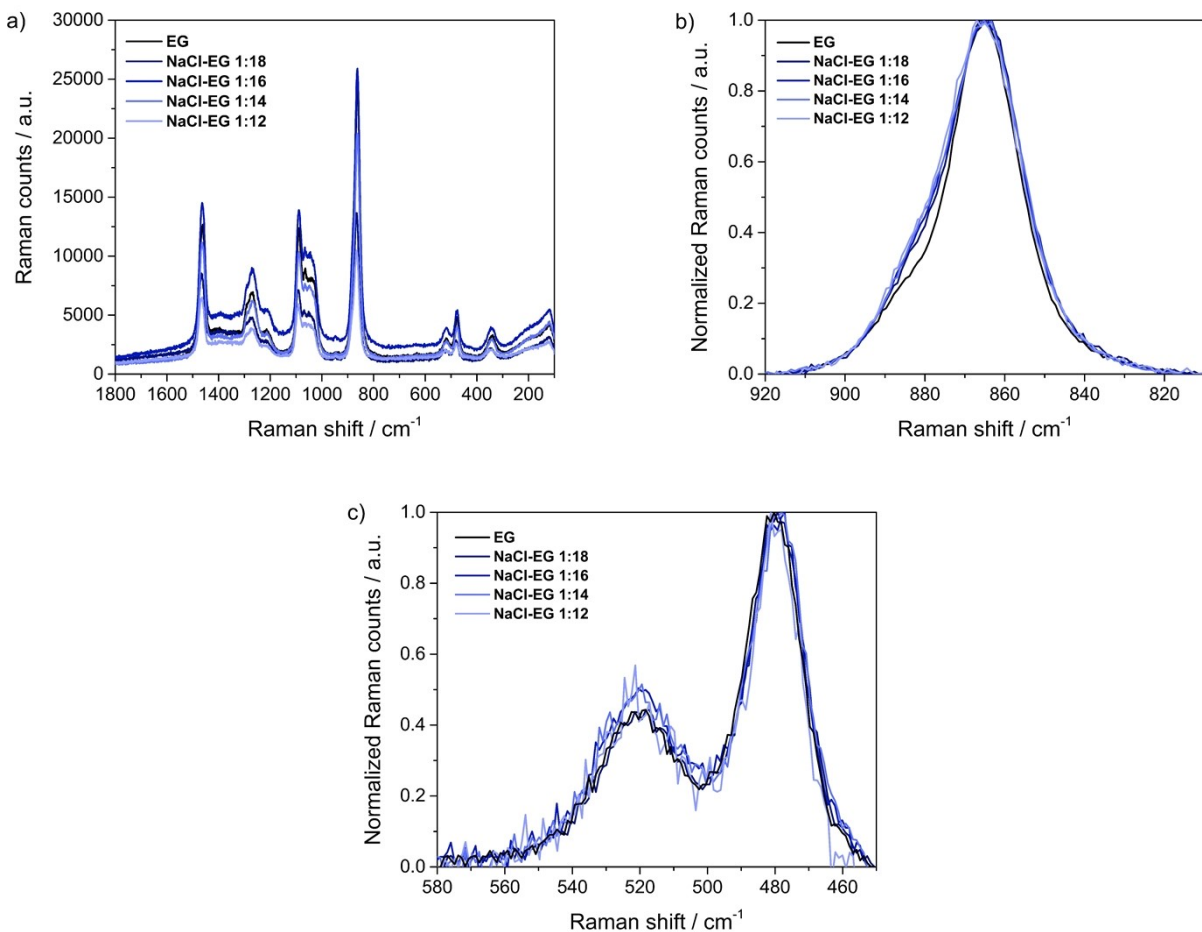


Figure S4. a) Experimental Raman spectra in the region $100\text{-}1800\text{ cm}^{-1}$ of pure EG and EG-based mixtures b) Normalised Raman spectra in the region $810\text{-}920\text{ cm}^{-1}$ c) Normalised Raman spectra in the region $450\text{-}580\text{ cm}^{-1}$.

Raman shift / cm^{-1}	Assignment
482	C-C-O bending (trans)
523	C-C-O bending (gauche)
865	C-C stretch
1043	C-O stretch (gauche)
1067	C-O stretch (trans)
1090	CH_2 rocking
1218	CH_2 twisting
1270	CH_2 twisting
1463	CH_2 scissoring

Table S5. Principal bands of ethylene glycol in the region $100\text{-}1800\text{ cm}^{-1}$ according to ⁸.

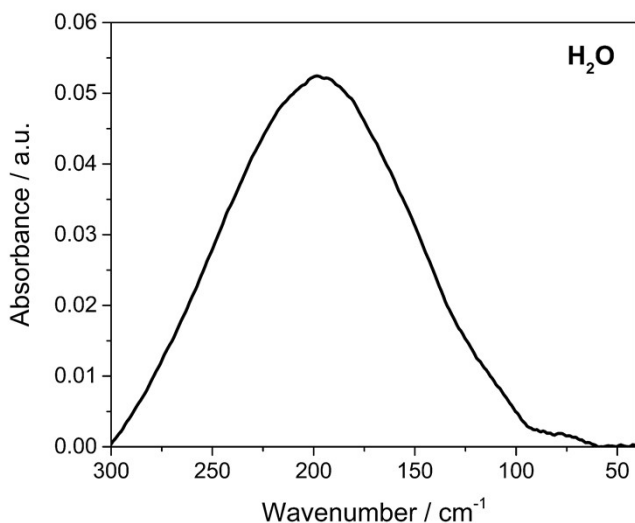


Figure S5. FIR spectrum of pure water.

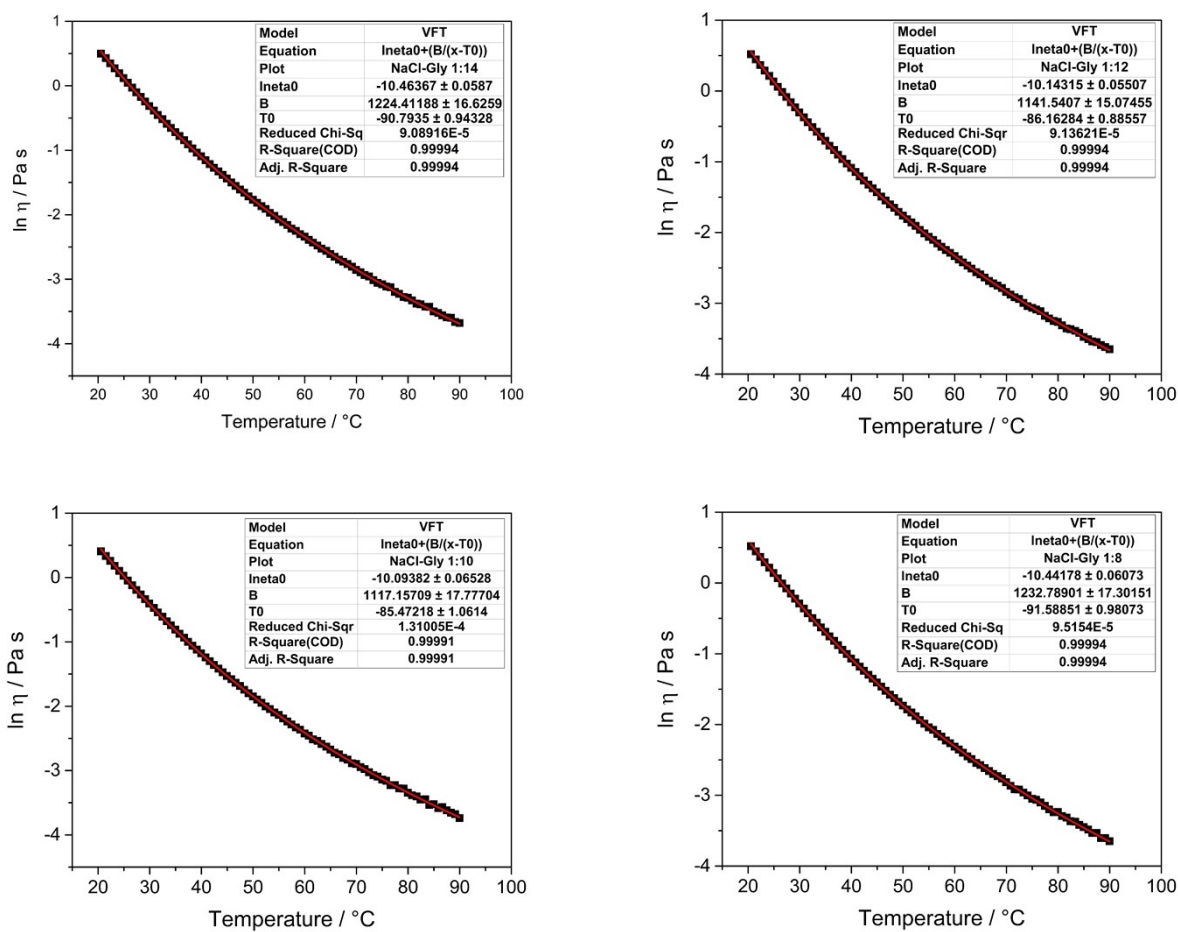


Figure S6. VFT fitting of NaCl-Gly viscosity curves.

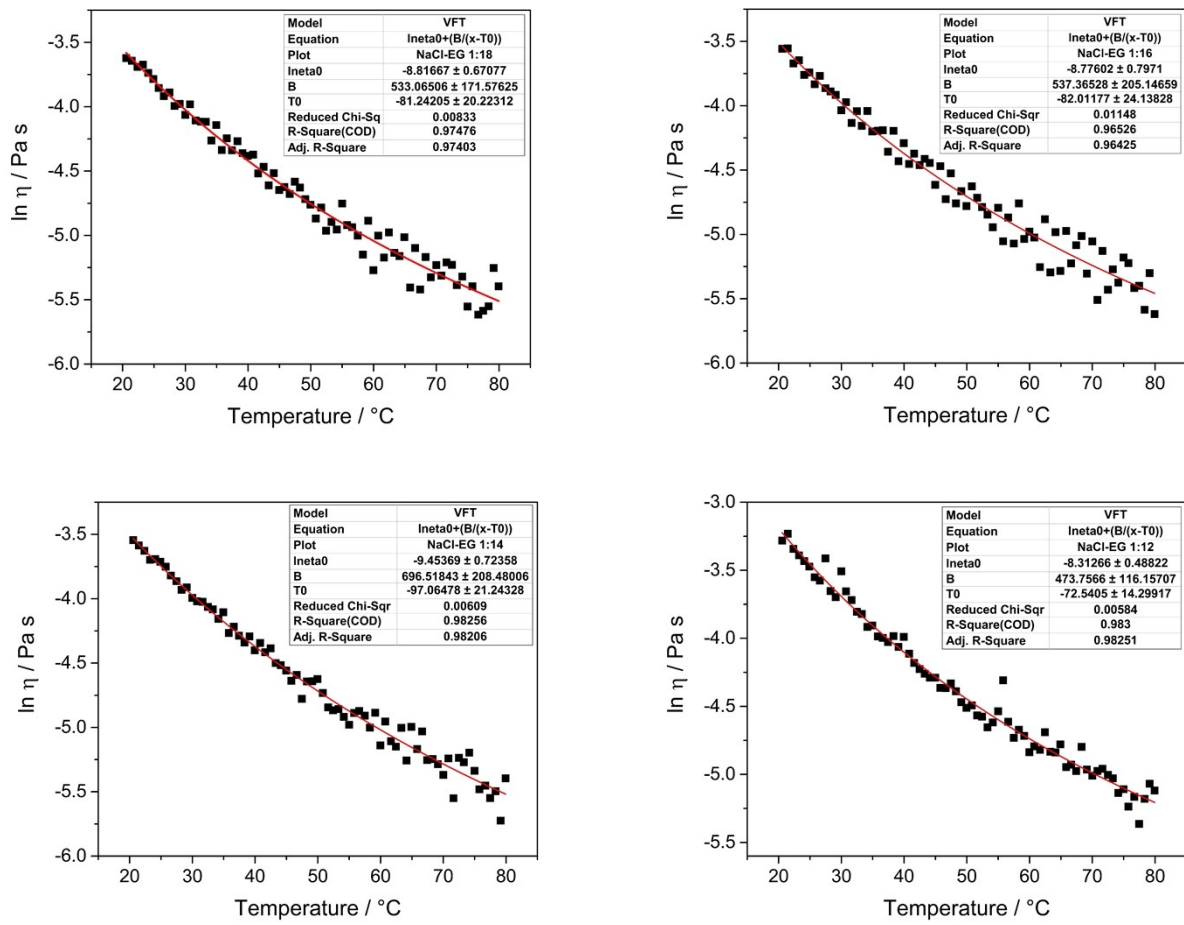


Figure S7. VFT fitting of NaCl-EG viscosity curves.

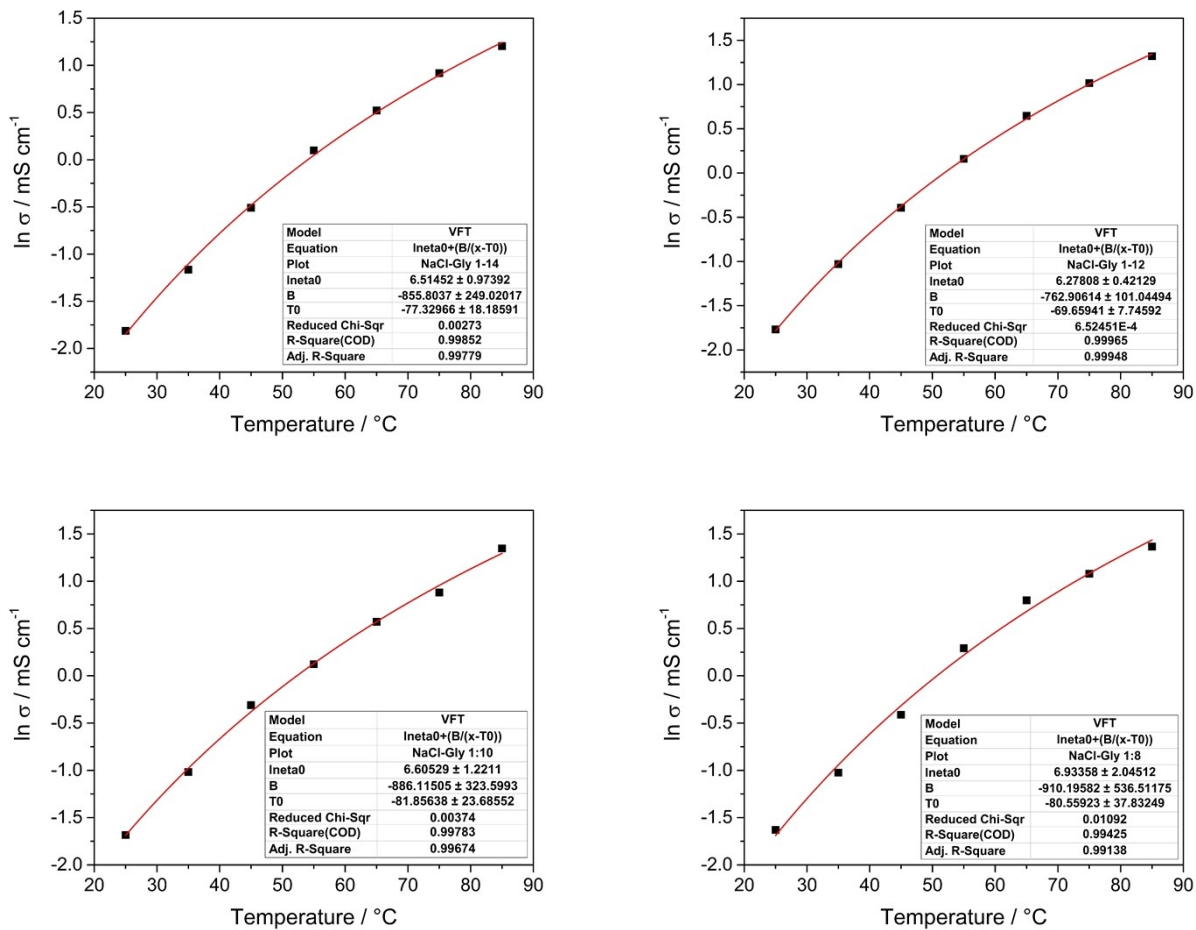


Figure S8. VFT fitting of NaCl-Gly ionic conductivity curves.

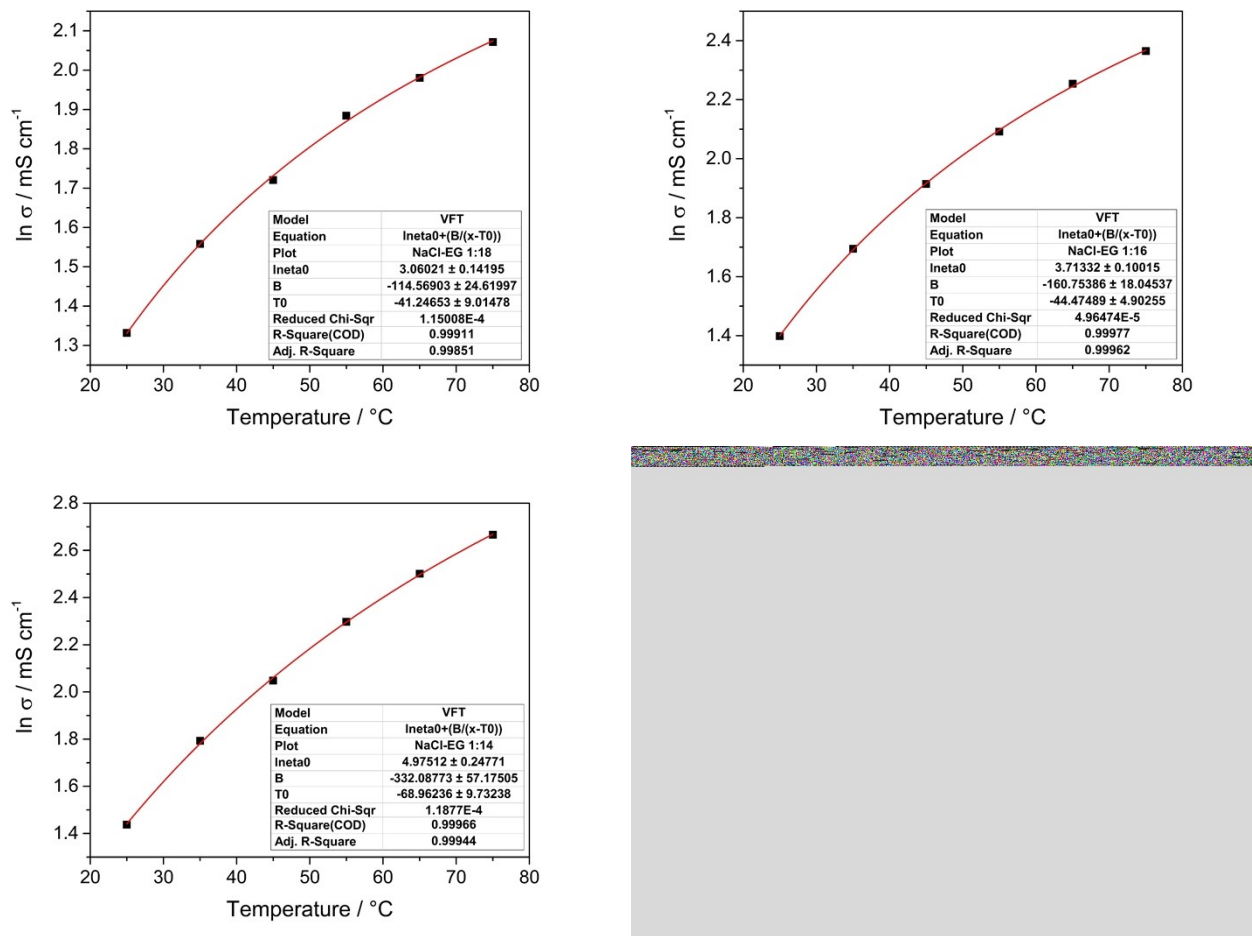


Figure S9. VFT fitting of NaCl-EG ionic conductivity curves.

Mixture	Molar ratio	η_0	B	T_0
		$mPa\ s$	$kJ\ mol^{-1}$	$^{\circ}C$
NaCl-EG	1:18	0.149 ± 0.002	533 ± 172	-81.2 ± 20.2
	1:16	0.153 ± 0.002	537 ± 205	-82.0 ± 24.1
	1:14	0.079 ± 0.002	697 ± 208	-97.0 ± 21.2
	1:12	0.245 ± 0.002	474 ± 116	-72.5 ± 14.3
NaCl-Gly	1:14	0.0286 ± 0.001	1224 ± 17	-90.8 ± 0.9
	1:12	0.0394 ± 0.001	1142 ± 15	-86.2 ± 0.9
	1:10	0.0415 ± 0.001	1117 ± 18	-85.5 ± 1.1
	1:8	0.0292 ± 0.001	1233 ± 17	-91.6 ± 1.0

Table S6. VFT coefficients obtained from the experimental viscosity curves.

Mixture	Molar ratio	σ_0	B	T_0
		$mS\ cm^{-1}$	$kJ\ mol^{-1}$	$^{\circ}C$
NaCl-EG	1:18	21.3 ± 1.2	-115 ± 25	-41.2 ± 9.0
	1:16	41.0 ± 1.1	-161 ± 18	-44.5 ± 4.9
	1:14	145 ± 1	-332 ± 57	-68.8 ± 9.7
	1:12	69.3 ± 1.3	-222 ± 47	-56.5 ± 10.6
NaCl-Gly	1:14	675 ± 3	-856 ± 249	-77.3 ± 18.2
	1:12	528 ± 2	-763 ± 101	-69.6 ± 7.7
	1:10	739 ± 3	-886 ± 324	-81.9 ± 23.7
	1:8	1026 ± 8	-910 ± 536	-80.6 ± 37.8

Table S7. VFT coefficients obtained from the experimental ionic conductivity curves.

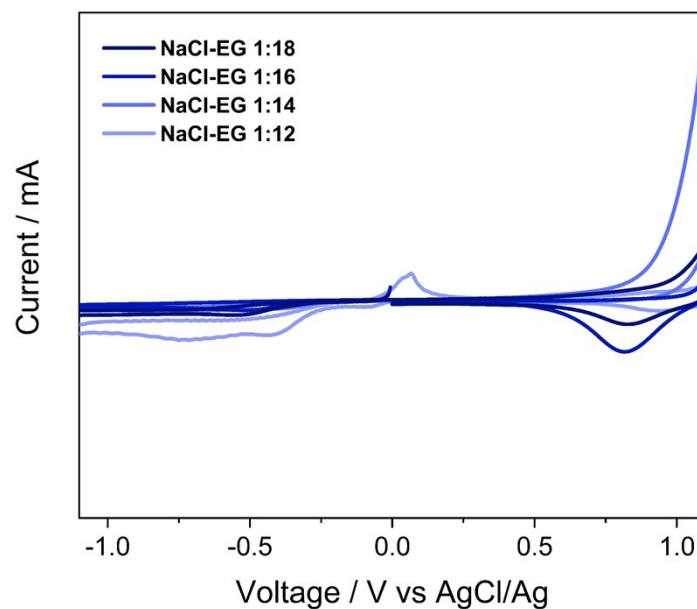


Figure S10. ESW detail showing faradic contributions in EG-based mixtures.

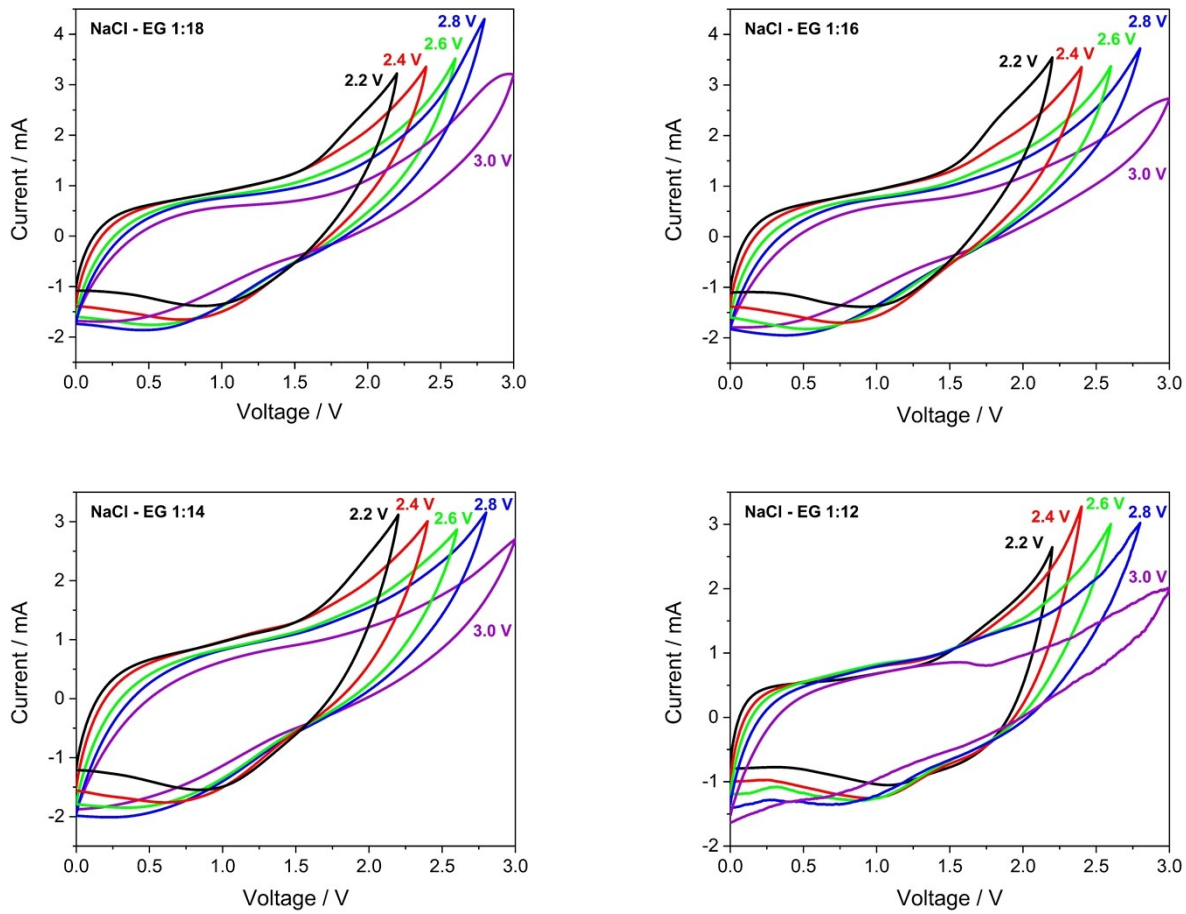


Figure S11. CV curves of NaCl-EG electrolytes in AC supercapacitors acquired at 1 mV s^{-1} with different operational voltages (2.2, 2.4, 2.6, 2.8, 3 V).

NaCl-Gly 1:10 post mortem

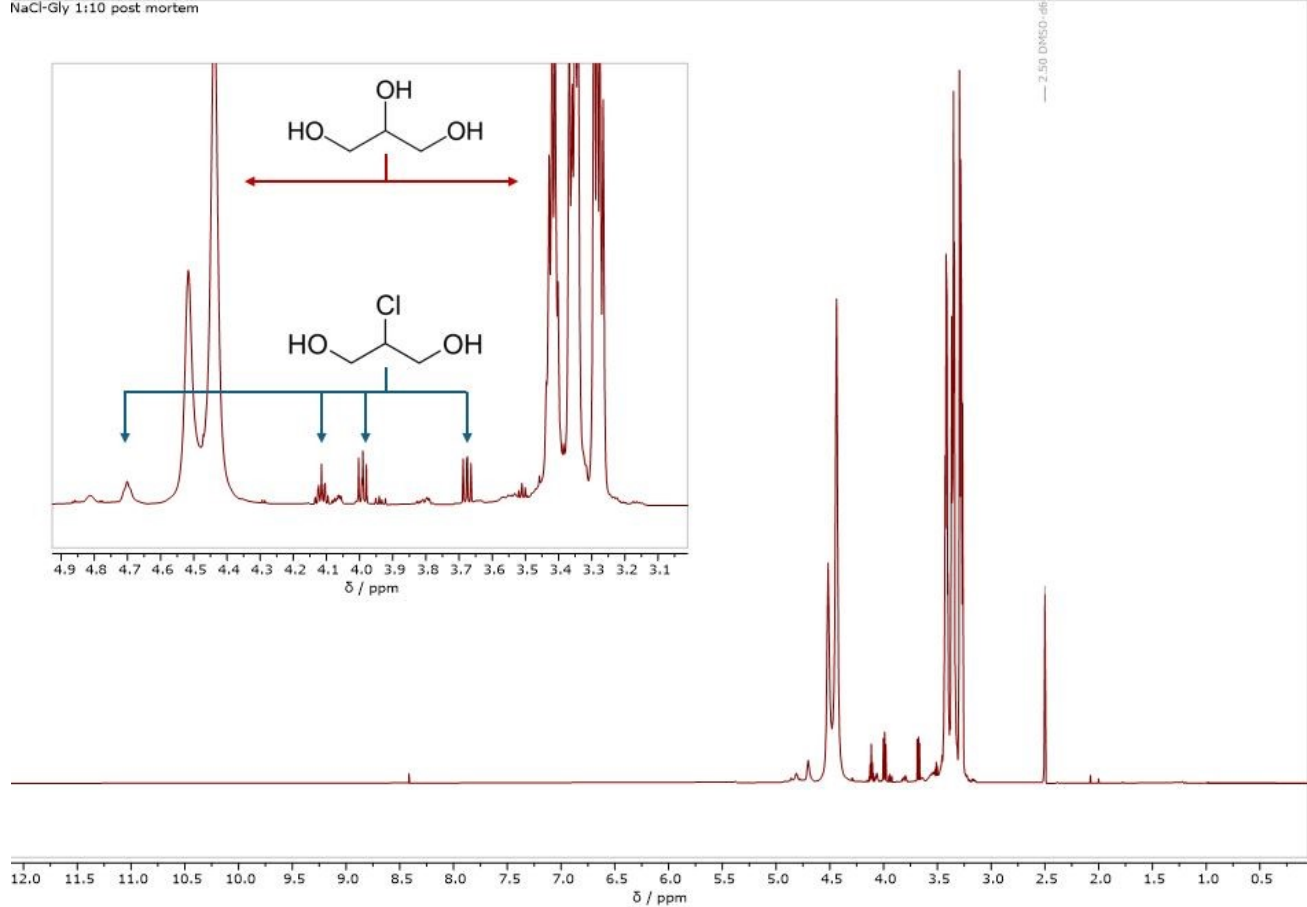


Figure S12. ^1H NMR spectrum of NaCl-Gly 1:10 post-cycling in EDLC.

References

- 1 M. J. Frisch, G. W. Trucks, H. B. Schlegel, G. E. Scuseria, M. A. Robb, J. R. Cheeseman, G. Scalmani, V. Barone, G. A. Petersson, H. Nakatsuji, X. Li, M. Caricato, A. V Marenich, J. Bloino, B. G. Janesko, R. Gomperts, B. Mennucci, H. P. Hratchian, J. V Ortiz, A. F. Izmaylov, J. L. Sonnenberg, D. Williams-Young, F. Ding, F. Lipparini, F. Egidi, J. Goings, B. Peng, A. Petrone, T. Henderson, D. Ranasinghe, V. G. Zakrzewski, J. Gao, N. Rega, G. Zheng, W. Liang, M. Hada, M. Ehara, K. Toyota, R. Fukuda, J. Hasegawa, M. Ishida, T. Nakajima, Y. Honda, O. Kitao, H. Nakai, T. Vreven, K. Throssell, J. A. Montgomery Jr., J. E. Peralta, F. Ogliaro, M. J. Bearpark, J. J. Heyd, E. N. Brothers, K. N. Kudin, V. N. Staroverov, T. A. Keith, R. Kobayashi, J. Normand, K. Raghavachari, A. P. Rendell, J. C. Burant, S. S. Iyengar, J. Tomasi, M. Cossi, J. M. Millam, M. Klene, C. Adamo, R. Cammi, J. W. Ochterski, R. L. Martin, K. Morokuma, O. Farkas, J. B. Foresman and D. J. Fox, GAUSSIAN 16 (Revision B.01), Gaussian Inc., Wallingford CT, 2016.
- 2 A. D. Becke, *J. Chem. Phys.*, 1993, **98**, 5648–5652.
- 3 C. Lee, W. Yang and R. G. Parr, *Phys. Rev. B*, 1988, **37**, 785–789.
- 4 S. Grimme, J. Antony, S. Ehrlich and H. Krieg, *J. Chem. Phys.*, 2010, **132**, 154104.
- 5 S. Grimme, S. Ehrlich and L. Goerigk, *J. Comput. Chem.*, 2011, **32**, 1456–1465.
- 6 A. V Marenich, C. J. Cramer and D. G. Truhlar, *J. Phys. Chem. B*, 2009, **113**, 6378–6396.
- 7 E. Mendelovici, R. L. Frost and T. Kloprogge, *J. Raman Spectrosc.*, 2000, **31**, 1121–1126.
- 8 A. Jindal and S. Vasudevan, *J. Phys. Chem. B*, 2021, **125**, 1888–1895.
- 9 A. Jindal and S. Vasudevan, *J. Phys. Chem. B*, 2017, **121**, 5595–5600.
- 10 R. M. Williams and R. H. Atalla, *J. Chem. Soc. Perkin Trans. 2*, 1975, 1155–1161.